Improved Pseudo-section Representation for CSAMT Data in Geothermal Exploration

Hendra Grandis[1*], **Prihadi Sumintadireja**[2]

[1]Applied and Exploration Geophysics Research Group, Faculty of Mining and Petroleum Engineering, Institut Teknologi Bandung, Jalan Ganesha 10 Bandung 40132, Indonesia
[2]Applied Geology Group, Faculty of Earth Science and Technology, Institut Teknologi Bandung, Jalan Ganesha 10 Bandung 40132, Indonesia

*corresponding author: grandis@itb.ac.id

Abstract. Controlled-Source Audio-frequency Magnetotellurics (CSAMT) is a frequency domain sounding technique employing typically a grounded electric dipole as the primary electromagnetic (EM) source to infer the subsurface resistivity distribution. The use of an artificial source provides coherent signals with higher signal-to-noise ratio and overcomes the problems with randomness and fluctuation of the natural EM fields used in MT. However, being an extension of MT, the CSAMT data still uses apparent resistivity and phase for data representation. The finite transmitter-receiver distance in CSAMT leads to a somewhat "distorted" response of the subsurface compared to MT data. We propose a simple technique to present CSAMT data as an apparent resistivity pseudo-section with more meaningful information for qualitative interpretation. Tests with synthetic and field CSAMT data showed that the simple technique is valid only for sounding curves exhibiting a transition from high – low – high resistivity (i.e. H-type) prevailing in data from a geothermal prospect. For quantitative interpretation, we recommend the use of the full-solution of CSAMT modelling since our technique is not valid for more general cases.

1. Introduction

Controlled-Source Audio-frequency Magnetotellurics (CSAMT) typically uses a grounded electric dipole as an artificial electromagnetic (EM) signal source operating in the 0.1 Hz to 10 kHz frequency band. With higher amplitude signals, better quality CSAMT data can be achieved relative to those from MT sounding that uses the natural EM source [1,2]. In most cases, only one grounded electric dipole (1-2 km in length) is used and positioned along the *x*-axis. A multi-channel receiver records the electric field simultaneously at several dipoles (E_x) along a profile and the perpendicular magnetic field (H_y) at the center of the array. Therefore, only scalar impedance $Z_{xy} = E_x/H_y$ is obtained. The distance between CSAMT sounding sites along a profile is limited to around 100 m due to the restriction in cable transmission (see Figure 1). With such measurement configuration, the CSAMT technique tends to have a good lateral resolution.

With finite transmitter - receiver distance (R, typically 2 to 8 km), the EM field surrounding the transmitter behaves as far field and near field. In the far-field, the uniform plane-wave assumption prevailing in MT with distant source is still valid for CSAMT. In this case $R > 4\delta$, δ is the skin depth for a uniform equivalent material underlying the measurement area. The near-field is typically defined

when $R < \delta$ and there is a transition between far field and near field [1,3]. In all cases, the apparent resistivity and phase derived from MT theory (i.e. Cagniard's equation) is used to convert the CSAMT scalar impedance into more meaningful information. The problem is that the apparent resistivity does not equal to the true resistivity of a homogeneous medium in the near field. For layered medium, the apparent resistivity curve does not exhibit the "correct" resistivity-depth variation of the subsurface. Therefore, qualitative interpretation of apparent resistivity sounding curves and pseudo-section from CSAMT data is less intuitive than its MT counterpart.

Several attempts were made to transform CSAMT data such that they represent adequately the resistivity variation with depth as in MT data. The term "near-field correction" emerged, although the possibility of such correction is debatable. The effort was driven mainly to be able to model CSAMT data using more commonly available MT modeling. Most of the techniques proposed are based on a generalization of the homogeneous medium response to non-homogeneous cases [4,5]. However, such generalization is not reliable especially for complex structures [e.g. 6,7]. This paper describes the recalculation of the apparent resistivity for CSAMT data along a profile such that they can be presented as a pseudo-section having better correlation with the resistivity structure. We start with nearly similar approach with the one proposed previously [4,5,6]. Then, we also introduce a semi-subjective method in the interpolation of apparent resistivity curve in the transition field. The resulting apparent resistivity curve will more likely represent the resistivity-depth variation of the subsurface.

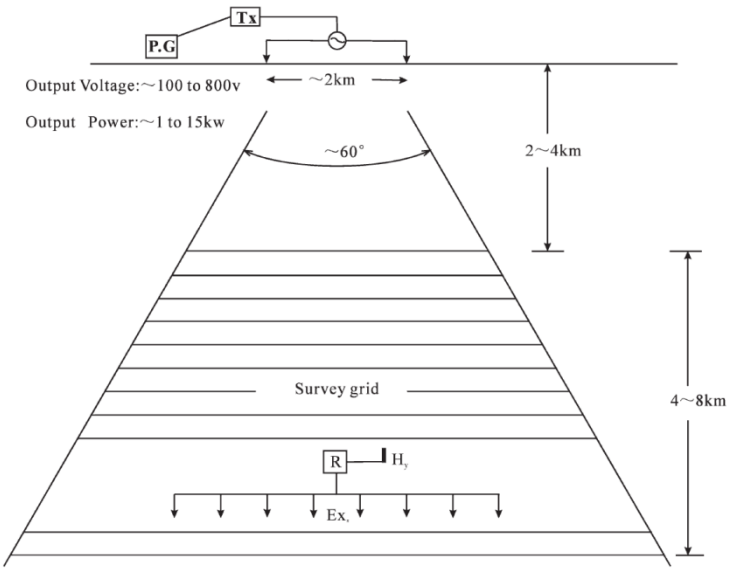

Figure 1. CSAMT field set-up with the electric dipole and transmitter (Tx) powered by an electrical power generator (PG). The receiver (R) records data from orthogonal components of electric and magnetic fields [1].

2. Far and near fields apparent resistivity

We performed MT and CSAMT 1D forward modeling using algorithms available in the literatures [8,9,10]. The so-called Cagniard's equation is commonly used to convert the MT complex scalar impedance Z_{xy} to apparent resistivity and phase. In a more generalized form with all quantities in SI units, the apparent resistivity equation used in both MT and CSAMT is,

$$\rho_a = \frac{1}{\omega\mu_0}\left|Z_{xy}\right|^2 \quad ; \quad \phi = \tan^{-1}\left(\frac{\mathrm{Im}\, Z_{xy}}{\mathrm{Re}\, Z_{xy}}\right) \tag{1}$$

where $\omega = 2\pi/T$, T is period (sec.) , μ_0 is the free-space magnetic permeability.

Figure 2 illustrates the differences between MT and CSAMT model response represented by the far field apparent resistivity and phase, i.e. equation (1) for simple layered models. We used the same 1D synthetic model with R = 2 km and R = 8 km. The model response exhibits an H-type sounding curves representing high - low - high resistivity variation with depth. In the far field, apparent resistivities for MT and CSAMT are identical up to T = 0.05 sec. for R = 2 km and to T = 0.15 sec. for R = 8 km. The near field prevails at longer periods where CSAMT apparent resistivity curves deviate and do not make an asymptote to the resistivity of the lowermost layer as for MT curves. The transition from far field to near field is usually identified by a "notch" represented by sharp resistivity change in a short interval of periods. Surprisingly, the "notch" appears only slightly with a shorter transmitter - receiver distance, i.e. R = 2 km. In all cases, a qualitative interpretation of apparent resistivity curves and pseudo-section from CSAMT data can be definitely misleading.

A more appropriate formula for the apparent resistivity in the near field can be used to obtain a sounding curve that might reflect the subsurface resistivity-depth variation. From the CSAMT response of a homogeneous medium [1], the the near field apparent resistivity can be calculated using,

$$\rho_a = 0.5\, R \left| Z_{xy} \right| \tag{2}$$

where R is the transmitter - receiver distance. Equation (2) is analogue to equation (1) in a sense that the apparent resistivity would be equal to the true resistivity of a homogeneous medium for near field and far field respectively. In the near field, the phase between electric and magnetic fields has no meaning since it falls almost strightly and makes an asymptote to 0^o (see Figure 2 lower panels).

Figure 3 shows apparent resistivity curves from far field equation (1) and near field equation (2) for the same synthetic models presented in Figure 2. The intersection between far field and near field apparent resistivities can be identified as the center of the transition between far field and near field (or "transition field" for short). However, the extent of the transition field from this center towards shorter and longer periods is not obvious. Even for the same models, the position in the horizontal axis (i.e. period) of the transition field depends on the transmitter - receiver or R. Therefore, more objective criteria have to be set if the "correction" will be applied to the transition zone.

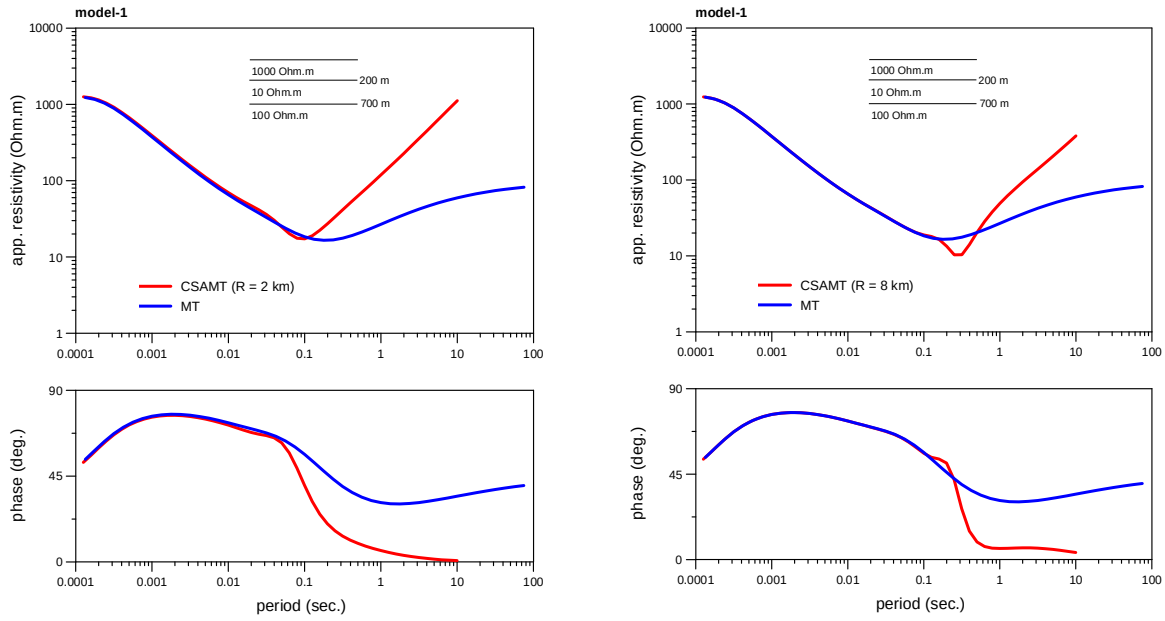

Figure 2. Apparent resistivity and phase curves from MT and CSAMT 1D forward modelling for a three-layered 1D model. R = 2 km (left) and R = 8 km (right) were used for CSAMT synthetic data.

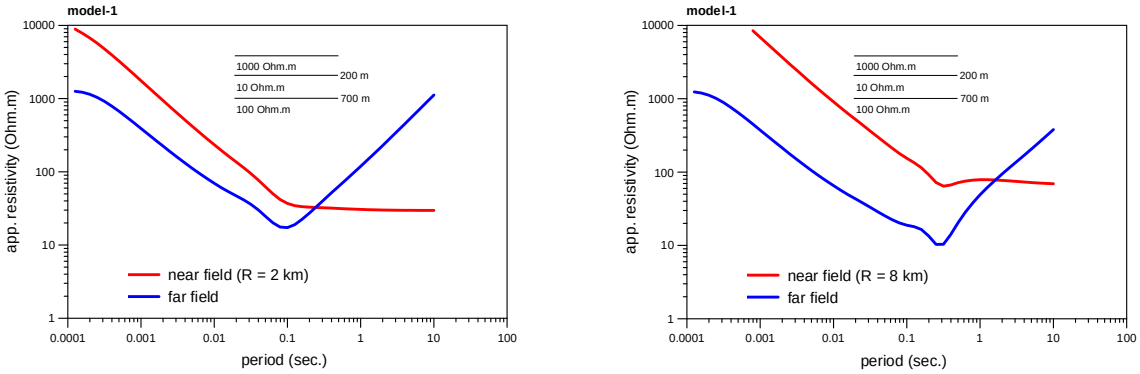

Figure 3. Apparent resistivity curves obtained from far field and near field equations for 1D synthetic models identical to those in Figure 3, with R = 2 km (left) and R = 8 km (right).

3. Transition field correction

In order to identify unambiguously the transition field, we study the characteristics of CSAMT response of a homogeneous medium and extend the results to more general cases, i.e. the non-homogeneous medium. The apparent resistivity curves for different homogeneous media with R = 2 km and R = 8 km are presented in Figure 4. Both transmitter - receiver distances represent the most commonly used field set-up in CSAMT. The curves are not plotted for all periods to avoid cluttering the figure. The transition from far field to near field is characterized by the deviation of apparent resistivity curves from the true resistivity of the homogeneous medium. The position of the transition field in the period axis depends both on the transmitter - receiver distance and the resistivity of the medium. In the resistive medium (e.g. 1000 Ohm.m) the far field extends only to short periods since the skin depth is large, and vice versa. In the same resistive medium, the far field extends towards longer periods for the larger transmitter- receiver distance (see Figure 4 right for R = 8 km).

To eliminate the dependence of the transition field on resistivity of the medium and transmitter - receiver distance, we propose to normalize the period as follows,

$$T^* = \frac{T}{R}\left|Z_{xy}\right| \tag{3}$$

where R is the transmitter - receiver distance in km, but we do not define the unit of T^* for simplicity.

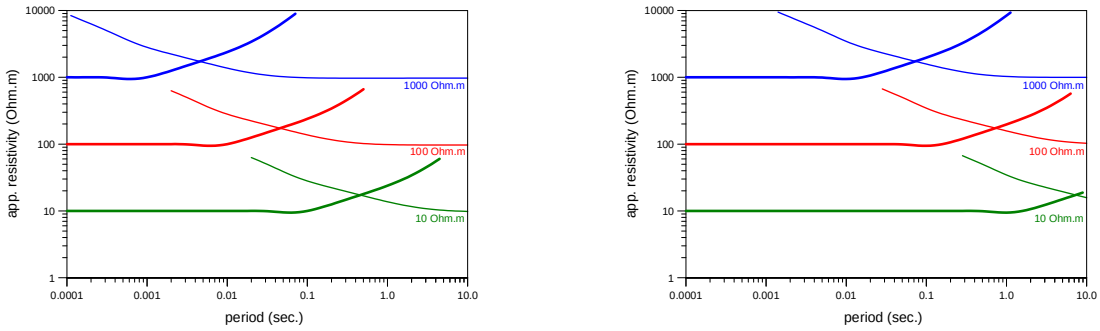

Figure 4. Apparent resistivity curves from far field equation (thick) and near field equation (thin) for different homogeneous media (10, 100 and 1000 Ohm.m) and transmitter - receiver distance, R = 2 km (left) and R = 8 km (right).

The apparent resistivity curves presented in Figure 4 are shown again in Figure 5 with the period transformed to the normalized period. It is obvious that the transition field position in the horizontal

axis does not depend on the resistivity of the medium and transmitter - receiver distance. In all cases the intersection between far field and near field apparent resistivity curves always occurs at $T^* = 0.004$ unit. This fact will certainly help in identifying the transition zone and its correction using factors defined in the next section. The apparent resistivity curves are not plotted for the entire periods for the sake of simplicity of the figure. However, the near field apparent resistivity curves stop at different normalized periods. The results of the transformation from period to normalized period using equation (3) differ for different resistivity of the medium and transmitter - receiver distance.

For a homogeneous medium, we can calculate the correction factor to transform the apparent resistivity in the transition field to become equal to the resistivity of the medium. The correction factor is equal to one in far and near fields, and deviates from unity in the transition field. These factors are independent from the resistivity of the medium and the transmitter - receiver distance as long as they are plotted in the normalized period axis (see Figure 6). The curves in Figure 6 are segments with different colors showing that they are plotted from exactly the same data as in Figure 4 and Figure 5. In the transition field, K_f and K_n are used to correct apparent resistivity curves of a homogeneous medium in the far field and near field sides respectively. Previously, the value of K_f and K_n are interpolated from a predefined table which may not be valid for general cases [4].

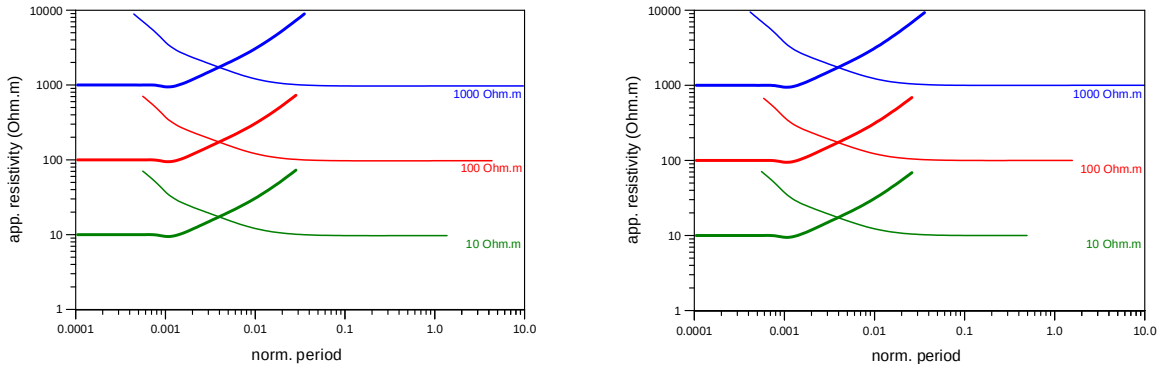

Figure 5. Apparent resistivity curves from far field equation (thin) and near field equation (thick) for different homogeneous media (10, 100 and 1000 Ohm.m) and transmitter - receiver distance R = 2 km (left) and R = 8 km (right). The normalized period is used in this figure.

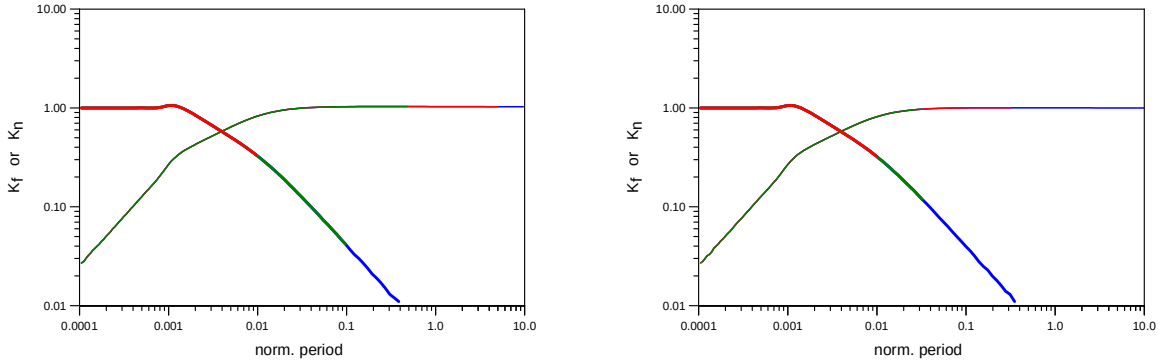

Figure 6. Correction factors for appparent resistivity curves from far field equation (thick) and near field equation (thin) to be equal to the resistivity of the medium for different homogeneous media (10, 100 and 1000 Ohm.m) and transmitter - receiver distance R = 2 km (left) and R = 8 km (right).

4. Results and discussion

The correction method for a homogeneous medium is considered valid and can be extended to CSAMT data associated with a non-homogeneous, i.e. layered medium. In the proposed technique, we

calculate CSAMT response of an arbitrary homogeneous medium, R and period interval. The resistivity of the medium and the period interval are chosen such that the resulting response are in a sufficiently large interval of the normalized period. Although it is not critical, R is chosen equal to the actual transmitter - receiver distance of the CSAMT data to be corrected. Then, K_f and K_n are calculated as function of the normalized period, from which the correction factors at the transition field of the CSAMT data are interpolated.

Figure 7 illustrates the results for synthetic data presented in Figure 2 and Figure 3. By comparing them with the MT synthetic data, it is obvious that the correction works relatively well, although it is not perfect. For the model with R = 2 km, the lowermost layer's resistivity is under-estimated. For the same model with R = 8 km, the "notch" still exists in the corrected curve. The result for synthetic data with other types of sounding curve, i.e. ascending or A-type and bell-shaped or K-type sounding curves, are not reliable and therefore the method is considered not applicable [e.g. 11].

The ability of the method to correct CSAMT data that exhibit high - low - high resistivity variation, i.e. H-type sounding curve, is important in geothermal exploration using CSAMT. This resistivity-depth variation represent the conductive clay cap sandwiched by the upper resistive layer mostly associated with volcanic products and the moderately resistive reservoir [12,13]. The un-corrected CSAMT data with very high resistivity at longer periods might falsely indicate shallower reservoir or thinner cap rocks. The correction made to the CSAMT data leads to the correct trend of resistivity-depth variations and a qualitative interpretation can be adequately based on the corrected data.

The method was applied to real (field) CSAMT data distributed along a profile from Kamojang geothermal area in West Java, Indonesia. At most of the sounding sites, the data exhibits very high resistivity at longer periods, which is typical with CSAMT data. However, the transmitter - receiver distance is only 2.5 km such that the "notch" is absent in the data as previously indicated by the synthetic data with a relatively short R. The result for representative sounding sites is presented in Figure 8. It is obvious that the method has successfully corrected the high resistivity at longer periods to become more reasonable. The corrected sounding curve equals to the original only at a very limited interval in periods which shows that most of the data are in transition and near fields. For all data on the profile, the comparison of the apparent resistivity pseudo-sections before and after correction also shows that the corrected pseudo-section appears to be more realistic in terms of the subsurface resistivity distribution (Figure 9). The geological implications of the CSAMT data are beyond the scope of the paper. Nevertheless, the information gained after the correction of the CSAMT data is of significant value. The cap rocks thickness and the reservoir depth would otherwise be under-estimated.

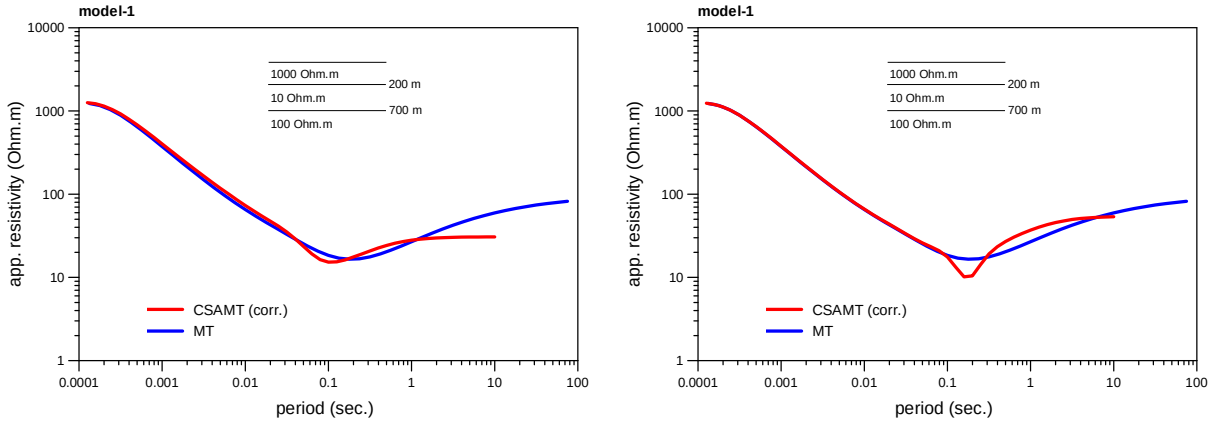

Figure 7. Synthetic CSAMT data with R = 2 km (left) and R = 8 km (right) after correction compared with the synthetic MT data of the same models (presented in Figure 2 and Figure 3).

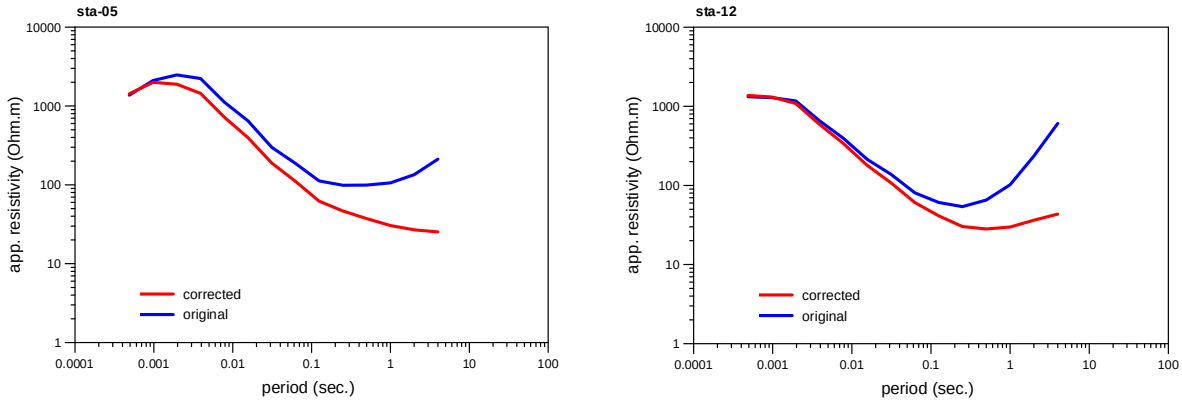

Figure 8. Result of CSAMT data correction from two sounding sites at Kamojang geothermal field, West Java, Indonesia.

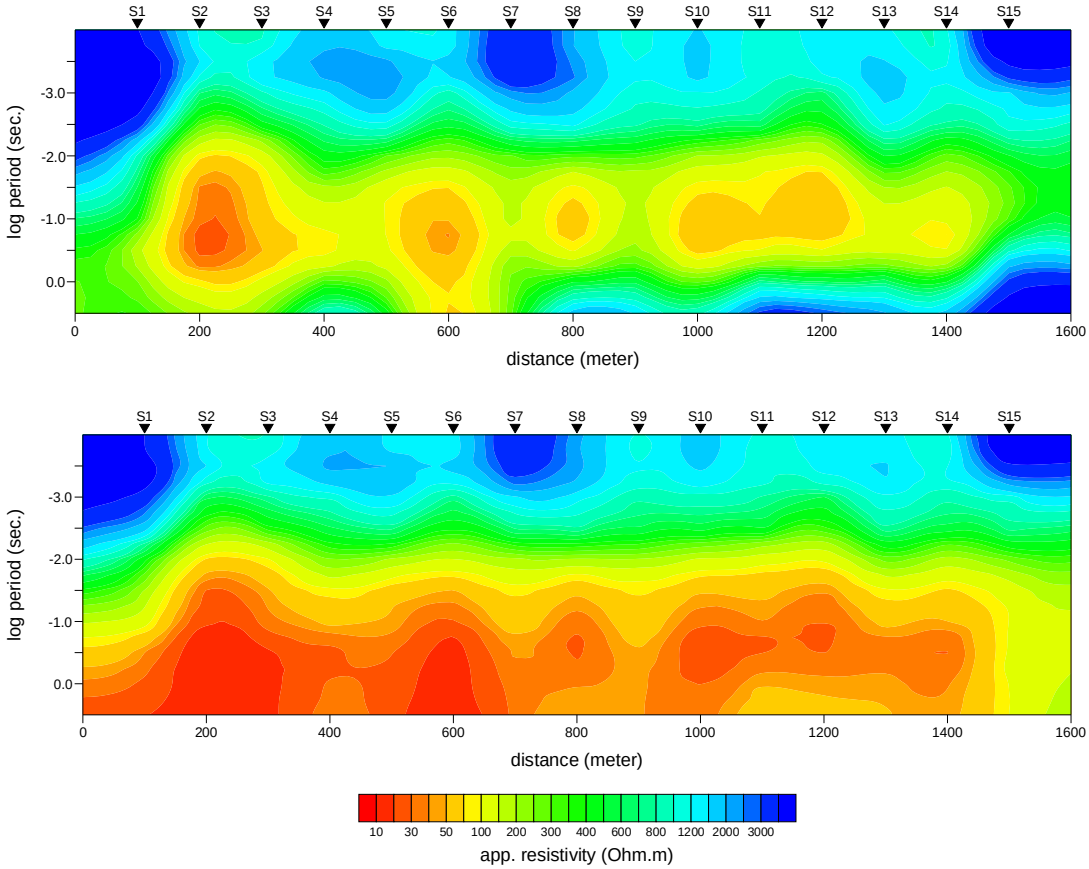

Figure 9. Apparent resistivity pseudo-sections of CSAMT data from Kamojang geothermal field, West Java, Indonesia, before (top panel) and after correction (lower panel) of the transition field. The apparent resistivity scale on the lower panel is for both pseudo-sections.

5. Conclusions

The CSAMT sounding technique appears to provide laterally high-resolution image of the subsurface thanks to the redundancy of the data along a profile line. However, CSAMT data and the pseudo-

section representation suffer from distortion effects due to the finite transmitter - receiver separation. Therefore, direct qualitative interpretation from uncorrected CSAMT data might be erroneous. We have presented a method for correcting CSAMT data which leads to a more reasonable resistivity-depth variation. The method is valid only for an H-type (and most probably Q-type or descending) CSAMT sounding curves prevailing mostly in CSAMT data from geothermal prospects. The applicability of the method was tested using synthetic and field data from a geothermal field with satisfactory results. The "notch" still exists in the data after correction, especially for CSAMT data with a large transmitter - receiver distance. This is a relatively negligible impact on the overall quality of the results.

The proposed method is intended only to produce a better apparent resistivity pseudo-section of CSAMT data for qualitative interpretation. The result with field data shows: (i) improved lateral continuity of the conductive layer, (ii) thicker and more pronounced (lower resistivity) conductive clay cap. For more quantitative interpretation, it is necessary to perform the so-called full solution for CSAMT forward and inverse modelling [3,9,10,14]. This will exonerate the need for the transition field correction presented in this paper. In the use of full solution modelling apparent resistivity pseudo-sections would serve only to compare observed and calculated values or data misfit.

References

[1] Zonge K L and L J Hughes 1991 Controlled-source audio-frequency magnetotellurics, in Nabighian M N (Ed.) Electromagnetic Methods in Applied Geophysics Vol. 2 *Society of Exploration Geophysicists*
[2] Zhdanov M S and G V Keller 1994 The geolectrical methods in geophysical exploration *Methods in Geochemistry and Geophysics* **31** Elsevier
[3] L Da, W Xiaoping, D Qingyun, W Gang, L Xiangrong, W Ruo, Y Jun and Y Mingxin 2016 *Journal of Geophysics and Engineering* **13** 49-58
[4] Grandis H 2000 *Jurnal Teknologi Mineral* **VII/1** 43-50.
[5] Yamashita M, P G Hallof and W H Pelton 1985 CSAMT case histories with a multi-channel CSAMT system and discussion of near-field data correction *55th SEG Annual Meeting Expanded Abstracts*
[6] Bartel L C and R D Jacobson 1987 *Geophysics* **52** 665-677
[7] Szarka L 1988 On "Results of a controlled-source audio-frequency magnetotelluric survey at Puhimau thermal area, Kilauea volcano Hawaii, by L.C. Bartel and R.D. Jacobson (Geophysics, 52, 665-677) *Geophysics* **53** 726-727
[8] Grandis H 1999 An alternative algorithm for one-dimensional magnetotelluric response calculation *Computer and Geosciences* **25** 119-125.
[9] Li X and L B Pedersen 1991 *Geophysics* **56** 1456-1461.
[10] Li X, B Oskooi and L B Pedersen 2000 *Geophysics* **65** 452-464.
[11] Grandis H and P Sumintadireja 2012 A brief review for the proper application of magnetotellurics (MT) and Controlled-Source Audio-frequency Magnetotellurics (CSAMT) in geothermal exploration *Proceedings of 12th Indonesian Geothermal Association Annual Meeting and Conference*
[12] Munoz G 2014 Exploring for geothermal resources with electromagnetic methods *Surveys in Geophysics* **35** 101-122.
[13] Armadillo E, D Rizzello, M Verdoya, C Pasqua and P Pisani 2015 Cubic spline regularization applied to 1D magnetotelluric inverse modeling in geothermal areas *Proceedings of World Geothermal Congress*
[14] Routh P and D W Oldenburg 1999 *Geophysics* **64** 1689-1697